
Article:
Sadabadi, M.S. (2021) Line-independent plug-and-play voltage stabilization and L2 gain performance of DC microgrids. IEEE Control Systems Letters, 5 (5). pp. 1609-1614.

https://doi.org/10.1109/lcsys.2020.3041335

Line-Independent Plug-and-Play Voltage Stabilization and $\mathscr{L}_2$ Gain Performance of DC Microgrids

Mahdieh S. Sadabadi

***Abstract*— The plug-and-play nature of distributed generation (DG) units in converter-interfaced microgrids imposes significant challenges from the control point of view, mainly caused by the time-varying microgrid structure. In this paper, we propose a systematic plug-and-play decentralized voltage control solution for DC microgrids. The proposed control approach guarantees the stable operation and satisfactory performance of microgrids under the arbitrary interconnection of DG units. Based on the Lyapunov method, concise stability and $\mathscr{L}_2$ gain voltage tracking performance certificates for DC microgrids are derived. The main feature of the proposed control approach is the decentralized design of local voltage controllers in DC microgrods. The proposed voltage control framework is applied to a case study of a multiple-DG DC microgrid in MATLAB/Simscape Electrical environment.**

***Index Terms*— DC microgrids, Plug-and-play voltage control, Stability and transient performance, $\mathscr{L}_2$ gain, Decentralized control.**

I. Introduction

Direct Current (DC) microgrids are drawing continually increasing attention over Alternating Current (AC) microgrids due to their advantages in higher efficiency, high reliability, reduced losses, and natural integration with renewable energy sources and energy storage resources [1]. With the recent advances in power electronics technologies, converter-interfaced DC microgrids are becoming more prevalent while posing a number of significant different control challenges. The challenges include stability issues due to the low-inertia characteristics of power electronics-based generations as well as uncertainties affecting the microgrid topology regarding system expandability, flexibility, and plug-and-play (PnP) functionality of distributed generation (DG) units. The plug-and-play operation of DG units affects the topology and global model of DC microgrids. However, the local loads in DC microgrids have to be stabilized without retuning the microgrid control system, in the absence of any communication link. Under the PnP functionality of DG units, classical control approaches which rely on a global model of the microgrids need to retune their control system in order to guarantee the stability of DC microgrid with a new topology. Therefore, due to importance of the plug-and-play problem in flexible and expandable microgrids, it is required to develop scalable control strategies for microgrids, where the design of a local controller for a DG unit is not based on the knowledge of the whole microgrid and the complexity of local control design is independent of the microgrid size. In a plug-and-play control system, the flexibility in the structure of the microgrids is reflected in the control architectures. As a result, when the microgrid topology changes, the control structure can be updated while ensuring the stable operation of the microgrids. A significant challenge in DC microgrids under the plug-and-play operation of DG units is to ensure voltage stability by means of the decentralized control of each DG unit [2].

The plug-and-play voltage control approaches in DC microgrids can be categorized as droop-based and non-droop-based control methods. The droop-based control category brings several advantages to microgrids including ease of implementation, expandability, and reliability with the plug-and-play feature [2], [3]. Despite the potential benefits of the droop-based control strategy, it comes at the cost of instability issues, slow dynamic responses, and dependency on the line impedance [4]. In recent years, non-droop-based control techniques have gained increasing popularity for voltage control of converter-interfaced DC microgrids. This class of microgrid control is based on advanced control approaches. Examples of these non-droop-based control approaches are [4]–[9] in which stabilizing PnP voltage control techniques have been developed. Although these approaches stabilize the voltage of DC microgrids, they do not guarantee that the transient behaviour of microgrids during the PnP operations of DG units is preserved. As a result, they might result in the poor system-wide performance of microgrids and cause performance deterioration under plug-in and/or plug-out of DG units. Unsatisfactory transient behaviour in islanded microgrids might lead to a risk of hardware damages because of equipment operating ranges and safety concerns. Yet, a systematic plug-and-play voltage control approach, which considers both stability and transient performance of microgrids, is highly desirable to facilitate the seamless integration and/or disconnection of any DG units without a need for redesigning the local voltage controllers.

Motivated by the aforementioned challenges and due to the importance of the transient response of voltages in microgrids,

Manuscript received September 5, 2020; revised November 7, 2020; accepted November 21, 2020.

M. S. Sadabadi is with the Department of Automatic Control and Systems Engineering, University of Sheffield, Sheffield, United Kingdom (e-mail: m.sadabadi@sheffield.ac.uk).

we develop a novel line-independent PnP voltage control approach that delivers the stable operation and satisfactory voltage-tracking performance of microgrids with flexible structures. In the proposed PnP voltage control technique, the design of decentralized PnP voltage controllers is formulated as a loop shaping control problem, which guarantees the satisfactory $\mathscr{L}_2$ gain voltage tracking performance of DC microgrids with dynamic resistive-inductive-capacitive lines. We show that the desired performance specifications in microgrids can be cast as a convex optimization problem with Linear Matrix Inequality (LMI) constraints. The solution of the optimization problem is in terms of a decentralized two-degree-of-freedom (2DOF) feedback-feedforward local voltage controller that fulfills specific $\mathscr{L}_2$ gain voltage tracking performance specifications. By virtue of this description and use of the results from the Lyapunov method, the stability and voltage-tracking performance specifications of DC microgrids under the PnP operation of DG units are preserved. One of the main features of our proposed control strategy is that the complexity of the proposed optimization problem grows linearly with the number of DG units, making the approach feasible to deal with large-scale problems.

The proposed control strategy in this paper offers the following main features: (i) The plug-and-play operation of DG units does not influence the stable operation and reliability of microgrids, this differs from [6], where the plug-in or plug-out of DG units requires the redesigning of all or neighbouring local voltage controllers. (ii) The proposed voltage control approach incorporates dynamic resistive-inductive-capacitive lines, which are neglected in [5]–[8]. (iii) The design of decentralized voltage controllers is decentralized and independent of the parameters and the bounds of distribution lines, which are required in [5], [6], [8]. (iv) The proposed voltage control method guarantees the stability and desired $\mathscr{L}_2$ gain voltage tracking performance of microgrids under the plug-and-play operation of DG units. This performance specification has not been considered in [4]–[9].

Notation: The notation used in this paper is standard. In particular, $\mathbf{0}_n$ is an $n\times 1$ zero vector and $\mathbf{I}_n$ is an $n\times n$ Identity matrix. The symbols X^T and $\star$ denote the transpose of matrix X and a symmetric term in a symmetric matrix. Throughout the paper, $\text{col}(x_i)=\begin{bmatrix} x_1^T & x_2^T & \dots & x_n^T \end{bmatrix}^T$ and $[a]=\text{diag}(a_1,a_2,\dots,a_n)$. For a symmetric matrix X, the positive definite and negative definite operators are respectively shown by $X\succ 0$ and $X\prec 0$. We define the sets $\mathbb{R}_{\geq 0}:=\{x\in\mathbb{R}\ \ |x\geq 0\}$ and $\mathbb{R}_{>0}:=\{x\in\mathbb{R}\ \ |x>0\}$. σ_{max} and σ_{min} denote the maximum and minimum singular value, respectively.

II. DC Microgrid Model

Consider a DC microgrid composed of n converter-interfaced DG units connected through m distribution lines. Each DG unit consists of a DC-DC buck converter, a resistive-inductive-capacitive filter with the parameters $(R_{t_i},L_{t_i},C_{t_i})$ and a local load connected at the Point Of Interconnection (POI). It is assumed that the loads at POIs are constant impedance. The energy source of each DG unit is represented by a DC voltage source $V_{dc,i}$. An electrical scheme of a DG unit is shown in Fig. 1.

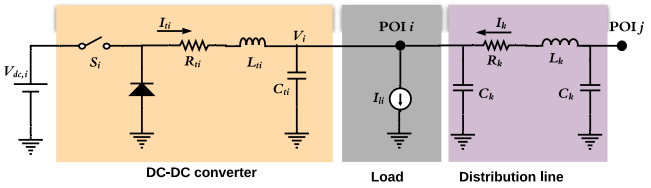

Fig. 1. A schematic diagram of DG i connected to DG j via line k.

DG Units Dynamics: The dynamics of the DG unit i are described as follows:

$$\begin{aligned} L_{t_i}\dot{I}_{t_i}(t) &= -R_{t_i}I_{t_i}(t)-V_i(t)+V_{dc_i}d_i(t),\\ \tilde{C}_{t_i}\dot{V}_i(t) &= I_{t_i}(t)-Y_iV_i(t)-\sum_{k=1}^{m}\mathscr{B}_{ik}I_k(t), \end{aligned} \tag{1}$$

where $\tilde{C}_{t_i}=C_{t_i}+\sum_{k=1}^{m}|\mathscr{B}_{ik}|C_k$, $V_i(t)\in\mathbb{R}$, $I_{t_i}(t)\in\mathbb{R}$, $d_i(t)\in\mathbb{R}$, $I_k(t)\in\mathbb{R}$, and $Y_i\in\mathbb{R}_{>0}$ are the voltage at POI i, the filter current, the duty cycle of DC-DC converter i, the distribution line current, and the load conductance, respectively. The term $\mathscr{B}_{ik}$ that defines the direction of the distribution line current is formulated as follows:

$$\mathscr{B}_{ik}=\begin{cases} 1 & \text{if line } k \text{ leaves DG } i,\\ -1 & \text{if line } k \text{ enters DG } i,\\ 0 & \text{otherwise.}\end{cases} \tag{2}$$

for $i=1,\dots,n$ and $k=1,\dots,m$.

Parameter Uncertainty in Shunt Capacitance $\tilde{C}_{t_i}$: Due to the plug-and-play operation of DG units, $\tilde{C}_{t_i}$ is subject to parameter uncertainties. In general, $\tilde{C}_{t_i}$ can be written as $\tilde{C}_{t_i}=C_{t_i}+\sum_{k\in\mathscr{N}_i}C_k$, where $\mathscr{N}_i$ is the set of lines connected at POI i which can vary over time. The variations in $\tilde{C}_{t_i}$ can be modeled as the following polytopic uncertainty matrix

$$\tilde{C}_{t_i}(\lambda)=\lambda\underline{C}_{t_i}+(1-\lambda)\bar{C}_{t_i},\quad 0\leq\lambda\leq 1, \tag{3}$$

where $\underline{C}_{t_i}=C_{t_i}$ and $\bar{C}_{t_i}=C_{t_i}+\sum_{k\in\mathscr{N}_{max_i}}C_k$, obtained from the total maximum possible case of the lines connected to POI i.

Line Dynamics: DG units are connected via distribution lines. In this letter, we focus on DC microgrids with a general resistive-inductive-capacitive line model (π-model [10]). Clearly, this can be applied to low-voltage DC networks which mainly have static (resistive) power lines, as well as medium-voltage and high-voltage DC microgrids where the power lines are not purely resistive and the line inductances are substantial [4]. The line k is modeled by the following equation:

$$L_k\dot{I}_k(t)=-R_kI_k(t)+\sum_{j=1}^{n}\mathscr{B}_{jk}V_j(t). \tag{4}$$

where (R_k,L_k) are the distribution line parameters.

III. Voltage Regulation in DC Microgrids

This section presents the voltage control problem in DC microgrids. The voltage control of microgrids is based on a hierarchical control mechanism composed of higher-level control, for instance a current-sharing scheme or a power management system, and primary control [7]. The main function of the higher-level control system is to maintain the optimal and efficient operation of microgrids [11] and determines appropriate voltage setpoints V_i^* for the primary control level. The primary control is equipped with local voltage regulators

that measure the voltage at their corresponding POIs and then provide the voltage tracking according to the reference setpoints.

The main objective of this paper is to design decentralized local voltage controllers for DG units that (i) guarantee the voltage stability and maintain the voltages at POIs within desired ranges $V_i^* \pm \Delta V_i$, where ΔV_i is usually around 10% of V_i^* [12]–[14], under the plug-and-play operation of DG units and (ii) fulfill desired voltage tracking performance specifications according to IEEE standards in [14] and in spite of the electrical coupling amongst DG units.

A. $\mathscr{L}_2$ Gain Voltage Tracking Performance Specifications

To achieve the aforementioned objectives and track the voltage references V_i^* based on desired reference tracking performance, the $\mathscr{L}_2$ gain of the error signal $e_i(t) = V_i^* - V_i(t)$ to the reference voltages V_i^* should be minimized. To this end, we formulate the desired voltage tracking performance of DC microgrid as a loop shaping problem, by shaping the closed-loop sensitivity transfer function. To achieve a certain closed-loop bandwidth and limit the impact of output disturbances on the voltage tracking error, the following $\mathscr{H}_\infty$ optimization problem is considered:

$$\min \quad \|W(s)S(s)\|_\infty, \tag{5}$$

where $S(s)$ is the sensitivity function describing the transfer function from the reference voltage V^* to the load voltage errors $V^* - V(t)$ and $W(s) = [W_i(s)]$ is a low-pass filter. The weighting filter $W(s)$ is designed based on desired reference tracking performance, according to IEEE standards in [14], and output disturbance rejection [15] (page 376). The main objective of (5) is to shape $S(s)$ such that $S(j\omega)$ is small in the low frequencies and large in high frequencies. The shaping of $S(j\omega)$ also helps in disturbance rejection as disturbances usually have frequency content concentrated in the low-frequency range.

A common choice of the weighting filter $W_i(s)$, $i = 1,\dots,n$, is given as:

$$W_i(s) = \frac{\frac{s}{M_i} + \omega_i^*}{s + \omega_i^* \varepsilon_i}, \tag{6}$$

where ω_i^* is the desired closed-loop bandwidth and M_i is the maximum peak value of the frequency response of the sensitivity function [15] (pp. 56-58). Choosing the parameter $\varepsilon_i << 1$ in (6) ensures approximate integral action with $S(0) \approx 0$ [15] (pp. 83-84). Furthermore, a large value of ω_i^* yields a fast voltage response [15]. The low-pass filter $W_i(s)$, $i \in \{1,\dots,n\}$, is represented in the state-space framework as follows:

$$\begin{aligned} \dot{v}_i(t) &= A_{w_i} v_i(t) + B_{w_i} e_i(t), \\ z_i(t) &= C_{w_i} v_i(t) + D_{w_i} e_i(t), \end{aligned} \tag{7}$$

where $e_i(t)$ is the voltage error signal, $v_i(t)$ is the state of the first-order weighting filter $W_i(s)$ in (6), and $z_i(t)$ is the performance output that is used to satisfy the loop-shaping characteristics of DC microgrid. The state-space matrices $A_{w_i} \in \mathbb{R}$, $B_{w_i} \in \mathbb{R}$, $C_{w_i} \in \mathbb{R}$, and $D_{w_i} \in \mathbb{R}$ are obtained from the transfer function $W_i(s)$ given in (6).

B. Structure of Proposed Local Voltage Controllers

We consider a two-degree-of-freedom (2DOF) feedback-feedforward voltage control framework with a decentralized architecture in the form of

$$u_i(t) = K_i x_i(t) + K_{i,f} V_i^*, \tag{8}$$

for $i = 1,\dots,n$, where $x_i(t) = [V_i(t)\ I_{t_i}(t)\ v_i(t)]^T \in \mathbb{R}^{3\times 1}$ and $K_i \in \mathbb{R}^{1\times 3}$ and $K_{i,f} \in \mathbb{R}$ are the feedback and the feedforward control gains, respectively. To design the control gains, obtain the dynamics of the weighted sensitivity function WS, and solve the $\mathscr{H}_\infty$ optimization problem in (5), in the following the dynamics of DG units is augmented with the dynamics of the weighting filters in (7).

Given a weighting filter $W_i(s)$ with the state-state model in (7), the augmented model of DG i is obtained as follows:

$$\begin{aligned} \dot{x}_i &= \big(A_{g_i}(\lambda) + B_i K_i\big)x_i + (B_{v_i} + B_i K_{i,f})V_i^* + B_{I_i}(\lambda)\sum_{k=1}^{m} \mathscr{B}_{ik} I_k, \\ \dot{I}_k(t) &= -\frac{R_k}{L_k} I_k(t) + \frac{1}{L_k}\sum_{j=1}^{n} \mathscr{B}_{jk} V_j(t), \\ z_i(t) &= C_{v_i} x_i(t) + D_{v_i} V_i^*, \end{aligned} \tag{9}$$

for $i = 1,\dots,n$ and $k = 1,\dots,m$, where

$$\begin{aligned} A_{g_i}(\lambda) &= \begin{bmatrix} -\frac{Y_i}{\tilde{C}_{t_i}(\lambda)} & \frac{1}{\tilde{C}_{t_i}(\lambda)} & 0 \\ -\frac{1}{L_{t_i}} & -\frac{R_{t_i}}{L_{t_i}} & 0 \\ -B_{w_i} & 0 & A_{w_i} \end{bmatrix}, \ B_i = \begin{bmatrix} 0 \\ \frac{1}{L_{t_i}} \\ 0 \end{bmatrix}, \ B_{v_i} = \begin{bmatrix} 0 \\ 0 \\ B_{w_i} \end{bmatrix}, \\ B_{I_i}(\lambda) &= \begin{bmatrix} -\frac{1}{\tilde{C}_{t_i}(\lambda)} \\ 0 \\ 0 \end{bmatrix}, \ C_{v_i} = \begin{bmatrix} -D_{w_i} & 0 & C_{w_i} \end{bmatrix}, \quad D_{v_i} = D_{w_i}. \end{aligned} \tag{10}$$

IV. Proposed Voltage Control Strategy

This section proposes a line-independent scalable voltage control design strategy for DC microgrids in (9). The proposed control approach originates from the idea of $\mathscr{L}_2$ gain minimization of the closed-loop microgrid in Section III and is formulated by a set of linear matrix inequalities.

A. Local Conditions Implying $\mathscr{L}_2$ Gain Minimization

If the coupling term $\sum_{k=1}^{m} \mathscr{B}_{ik} I_k(t)$ in (9) is zero, the $\mathscr{H}_\infty$ certificate $\|W(s)S(s)\|_\infty \le \gamma$ can be achieved by simply minimizing the $\mathscr{H}_\infty$ norm of the closed-loop model of each DG. In the following, it is shown that under some specific conditions stated in the following assumption, the design of local voltage controller for each DG in a no-coupling case is a sufficient condition for the $\mathscr{L}_2$ gain minimization of the overall DC microgrid in (9) with couplings amongst the DG units.

Assumption 1: $K_{i,f}$, G_i, and $H_i = K_i G_i$ are designed using the following linear matrix inequality (LMI) condition:

$$\begin{bmatrix} A_i G_i + G_i A_i^T + B_i H_i + H_i^T B_i^T & \star & \star \\ (B_{v_i} + B_i K_{i,f})^T & -\gamma_i^2 & \star \\ C_{v_i} G_i & D_{v_i} & -1 \end{bmatrix} \prec 0. \tag{11}$$

for $i = 1,\dots,n$, where

$$G_i = \left[\begin{array}{c|c} \eta & \mathbf{0}_2^T \\ \hline \mathbf{0}_2 & \mathscr{G}_i \end{array}\right], \ A_i = \begin{bmatrix} -Y_i & 1 & 0 \\ -\frac{1}{L_{t_i}} & -\frac{R_{t_i}}{L_{t_i}} & 0 \\ -B_{w_i} & 0 & A_{w_i} \end{bmatrix} \tag{12}$$

where $\eta \in \mathbb{R}_{>0}$ and $\mathscr{G}_i \in \mathbb{R}^{2\times 2} \succ 0$.

Remark 1: The block-diagonal structure of G_i in (12) is a source of conservatism in the LMI constraints in (11). However, it is the price to convert the voltage control design problem to a scalable line-independent design approach.

Considering Assumption 1, the main results of this letter are presented in the following theorem:

Theorem 1: Let Assumption 1 holds. The conditions in (11) guarantees that $\|W(s)S(s)\|_\infty \leq \gamma$, $\gamma = \max_{i\in\{1,\ldots,n\}} \gamma_i$, for the overall DC microgrid in (9)-(10) under the plug-and-play operation of DG units.

Proof: We propose the following quadratic Lyapunov function $\mathscr{V}$ for the overall microgrid system in (9)-(10):

$$\mathscr{V} = \sum_{i=1}^{n} x_i^T(t) P_i(\lambda) x_i(t) + \frac{1}{\eta}\sum_{k=1}^{m} I_k^T(t) L_k I_k(t), \tag{13}$$

where $P_i(\lambda) \succ 0$ is structured as follows:

$$P_i(\lambda) = \left[\begin{array}{c|c} \frac{1}{\eta}\tilde{C}_{t_i}(\lambda) & \mathbf{0}_2^T \\ \hline \mathbf{0}_2 & \rho_i \end{array}\right], \ \rho_i = \mathscr{G}_i^{-1}. \tag{14}$$

The time derivative of $\mathscr{V}$ along the closed-loop trajectories in (9) is obtained as follows:

$$\begin{aligned}\dot{\mathscr{V}} &= \sum_{i=1}^{n} x_i^T Q_i(\lambda) x_i \\ &+ \sum_{i=1}^{n}\left(x_i^T P_i(\lambda) B_{I_i}(\lambda)\sum_{k=1}^{m}\mathscr{B}_{ik} I_k + \sum_{k=1}^{m} I_k^T \mathscr{B}_{ik} B_{I_i}^T(\lambda) P_i(\lambda) x_i\right) \\ &+ \sum_{i=1}^{n} x_i^T P_i(\lambda)(B_{v_i} + B_i K_{i,f}) V_i^* + \sum_{i=1}^{n} V_i^*(B_{v_i} + B_i K_{i,f})^T P_i(\lambda) x_i \\ &- \frac{2}{\eta}\sum_{k=1}^{m} I_k^T R_k I_k + \frac{1}{\eta}\sum_{k=1}^{m}\left(\sum_{j=1}^{n} I_k^T \mathscr{B}_{jk} V_j + \sum_{j=1}^{n} V_j^T \mathscr{B}_{jk}^T I_k\right),\end{aligned} \tag{15}$$

where $Q_i(\lambda) = (A_{g_i}(\lambda) + B_i K_i)^T P_i(\lambda) + P_i(\lambda)(A_{g_i}(\lambda) + B_i K_i)$. By direct calculation and invoking the specific structure of $P_i(\lambda)$ in (14), it yields that

$$\begin{aligned}&\sum_{i=1}^{n}\left(x_i^T P_i(\lambda) B_{I_i}(\lambda)\sum_{k=1}^{m}\mathscr{B}_{ik} I_k + \sum_{k=1}^{m} I_k^T \mathscr{B}_{ik} B_{I_i}^T(\lambda) P_i(\lambda) x_i\right) \\ &\quad + \frac{1}{\eta}\sum_{k=1}^{m}\left(\sum_{j=1}^{n} I_k^T \mathscr{B}_{jk} V_j + \sum_{j=1}^{n} V_j^T \mathscr{B}_{jk}^T I_k\right) = 0.\end{aligned} \tag{16}$$

Therefore, $\dot{\mathscr{V}}$ can be rewritten as follows:

$$\begin{aligned}\dot{\mathscr{V}} &= \sum_{i=1}^{n} x_i^T Q_i(\lambda) x_i - \frac{2}{\eta}\sum_{k=1}^{m} I_k^T R_k I_k + \sum_{i=1}^{n} x_i^T P_i(\lambda)(B_{v_i} + B_i K_{i,f}) V_i^* \\ &+ \sum_{i=1}^{n} V_i^{*T}(B_{v_i} + B_i K_{i,f})^T P_i(\lambda) x_i.\end{aligned} \tag{17}$$

Since $\eta > 0$ and $-I_k^T R_k I_k \leq 0$, one obtains that

$$\dot{\mathscr{V}} \leq \sum_{i=1}^{n}\begin{bmatrix} x_i \\ V_i^* \end{bmatrix}^T \begin{bmatrix} Q_i(\lambda) & P_i(\lambda)(B_{v_i} + B_i K_{i,f}) \\ \star & 0 \end{bmatrix}\begin{bmatrix} x_i \\ V_i^* \end{bmatrix}. \tag{18}$$

Moreover, by direct calculation it can be shown that

$$\begin{bmatrix} Q_i(\lambda) & \star \\ (B_{v_i} + B_i K_{i,f})^T P_i(\lambda) & 0 \end{bmatrix} = \begin{bmatrix} Q_{n_i} & \star \\ (B_{v_i} + B_i K_{i,f})^T G_i^{-1} & 0 \end{bmatrix}. \tag{19}$$

where $Q_{n_i} = G_i^{-1}(A_i + B_i K_i) + (A_i + B_i K_i)^T G_i^{-1}$ and (G_i, A_i) are defined in (12). As a result,

$$\dot{\mathscr{V}} \leq \sum_{i=1}^{n}\begin{bmatrix} x_i \\ V_i^* \end{bmatrix}^T \begin{bmatrix} Q_{n_i} & \star \\ (B_{v_i} + B_i K_{i,f})^T G_i^{-1} & 0 \end{bmatrix}\begin{bmatrix} x_i \\ V_i^* \end{bmatrix}. \tag{20}$$

Since Assumption 1 holds, the inequality condition in (11) is satisfied. It can be shown that the condition in (11) is equivalent to the existence of $\varepsilon_i \in \mathbb{R}_{>0}$ such that the following inequality, referred to as dissipation inequality [16] (page 45), is satisfied:

$$\begin{aligned}&\begin{bmatrix} x_i \\ V_i^* \end{bmatrix}^T \begin{bmatrix} Q_{n_i} & G_i^{-1}(B_{v_i} + B_i K_{i,f}) \\ \star & 0 \end{bmatrix}\begin{bmatrix} x_i \\ V_i^* \end{bmatrix} \\ &\qquad \leq \left(-\varepsilon_i x_i^T x_i + \gamma_i^2 V_i^{*T} V_i^* - z_i^T z_i\right).\end{aligned} \tag{21}$$

As a result, $\dot{\mathscr{V}} \leq \sum_{i=1}^{n}\left(-\varepsilon_i x_i^T x_i + \gamma_i^2 V_i^{*T} V_i^* - z_i^T z_i\right)$. Therefore, one obtains that

$$\dot{\mathscr{V}} \leq -\varepsilon x^T x + \gamma^2 V^{*T} V^* - z^T z, \tag{22}$$

where $\gamma = \max_{i\in\{1,\ldots,n\}} \gamma_i$ and $\varepsilon = \min_{i\in\{1,\ldots,n\}} \varepsilon_i$. The above dissipation inequality implies that $\|W(s)S(s)\|_\infty \leq \gamma$. ■

B. Plug-and-Play Design of Local Voltage Controllers

Considering the set of linear matrix inequities given in (11), K_i and $K_{i,f}$ are obtained from the following convex optimization problem:

$$\min_{\eta,\beta_i,\delta_i,\gamma_i,H_i,\mathscr{G}_i,K_{i,f}} \quad \alpha_{1,i}\gamma_i + \alpha_{2,i}\beta_i + \alpha_{3,i}\delta_i$$

subject to

$$\begin{bmatrix} A_i G_i + G_i A_i^T + B_i H_i + H_i^T B_i^T & \star & \star \\ (B_{v_i} + B_i K_{i,f})^T & -\gamma_i^2 & \star \\ C_{v_i} G_i & D_{v_i} & -1 \end{bmatrix} \prec 0, \tag{23a}$$

$$G_i = \left[\begin{array}{c|c} \eta & \mathbf{0}_2^T \\ \hline \mathbf{0}_2 & \mathscr{G}_i \end{array}\right] \succ 0, \tag{23b}$$

$$\begin{bmatrix} G_i & \mathbf{I}_3 \\ \mathbf{I}_3 & \delta_i \mathbf{I}_3 \end{bmatrix} \succ 0, \quad \begin{bmatrix} -\beta_i \mathbf{I}_3 & H_i^T \\ H_i & -1 \end{bmatrix} \prec 0. \tag{23c}$$

for $i = 1,\ldots,n$, where $\alpha_{1,i}$, $\alpha_{2,i}$, and $\alpha_{3,i}$ are positive weights characterizing a trade-off between the voltage tracking performance and the norm of the control gains. By solving the convex optimization problem in (23), the feedforward gain $K_{i,f}$ is obtained. The feedback gain of the voltage control is expressed as $K_i = H_i G_i^{-1}$.

Remark 2: The LMI constraints in (23c) penalize aggressive control actions and make the feedback control gains norm-bounded as $\|K_i\|_2 \leq \sqrt{\beta_i}\delta_i$ [6].

Remark 3: (*Plug-and-Play Operation of DG Units*) The line-independent and scalable properties of the proposed control strategy provides a plug-and-play feature where DGs units can be connected or disconnected over the time. When DG j, $j \in \{1,\ldots,n\}$, with the $\mathscr{L}_2$ gain γ_j is unplugged, the microgrid stability and voltage tracking performance with the $\mathscr{L}_2$ gain of $\max_{i\in\{1,\ldots,n\};i\neq j} \gamma_i$ are preserved. In the case that a new DG, let's say DG $n+1$ is plugged into DC microgrid, the microgrid remains stable. Furthermore, the $\mathscr{L}_2$ gain voltage tracking performance level changes to $\max(\gamma, \gamma_{n+1})$, provided that the DG $n+1$ has an $\mathscr{L}_2$ gain of γ_{n+1}. Note that the optimization problem in (23) is $\tilde{C}_{t_i}(\lambda)$-independent.

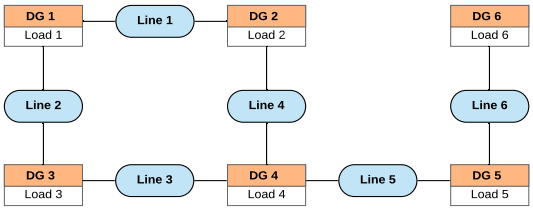

Fig. 2. Layout of DC microgrid under study.

Remark 4: (*Robustness to Parameter Uncertainty in Load Conductance*) In the case of the parameter uncertainty in the load conductance Y_i, $i \in \{1,\dots,n\}$, i.e. $\underline{Y}_i \le Y_i \le \bar{Y}_i$, matrix A_i in (12) has a polytopic uncertainty with two vertices. The vertices A_i^j, $i \in \{1,\dots,n\}$ and $j = 1,2$, are built by replacing Y_i in A_i by $\underline{Y}_i$ and $\bar{Y}_i$. In this case, we can show that $\|W(s)S(s)\|_\infty \le \gamma$ for all values of Y_i in the uncertainty interval if the condition given in (11) is satisfied for both A_i^1 and A_i^2 with a common H_i, $K_{i,f}$, and G_i as structured in (12).

C. Analysis of Steady-state Errors in Voltage Tracking

We recall that $E(s) = S(s)V^*(s)$, where $E(s)$ and $V^*(s)$ are the Laplace transform of the voltage error $e(t)$ and the voltage setpoint and $S(s)$ is the sensitivity function defined in Section III. According to the final value theorem, it can be shown that steady-state error of $e(t)$ to constant reference setpoints V^* can be obtained as follows:

$$e_{ss} = \lim_{t\to\infty} e(t) = S(0)V^*. \tag{24}$$

Furthermore, it can be shown that

$$\|e_{ss}\|_2 \le \sigma_{max}(S(0))\|V^*\|_2. \tag{25}$$

Small steady-state errors are guaranteed if $\sigma_{max}(S(0))$ is sufficiently small. In the proposed method in this letter, $\sigma_{max}(S(j\omega))$ is minimized in low frequencies by considering the cost function $\|W(j\omega)S(j\omega)\|_\infty$ in (5). In fact, $\|W(j\omega)S(j\omega)\|_\infty \le \gamma$ implies that the following condition is satisfied [17] (Chapter 20):

$$\sigma_{max}(S(j\omega)) \le \frac{\gamma}{\sigma_{min}(W(j\omega))},\ \forall\omega. \tag{26}$$

The above inequality holds for all frequencies including $\omega = 0$ which is the frequency of our interest. Since $W(0) = \text{diag}\left(\frac{1}{\varepsilon_1},\dots,\frac{1}{\varepsilon_n}\right)$ (Equation (6)), $\sigma_{min}(W(0)) = \frac{1}{\varepsilon_{max}}$, where $\varepsilon_{max} = \max_{i\in\{1,\dots,n\}} \varepsilon_i$. Therefore, $\sigma_{max}(S(0)) \le \gamma\varepsilon_{max}$. As a result,

$$\|e_{ss}\|_2 \le \gamma\varepsilon_{max}\|V^*\|_2. \tag{27}$$

If ε_i in $W_i(s)$ in (6) is chosen to be zero, $\varepsilon_{max} = 0$. Therefore $\sigma_{max}(S(0)) = 0$ and $e_{ss} = 0$. This guarantee integral action in the voltage controllers [17] (Chapter 20). However, to avoid numerical problems in the control design, ε_i is usually chosen to have a small positive value [15] (page 60). Selecting $\varepsilon_i << 1$ in $W_i(s)$ in (6) and minimizing γ via the optimization problem (23) make $\gamma\varepsilon_{max}$ very small. Hence, it ensures approximate integral action with $S(0) \approx 0$ ([15] (pp. 83-84)) and therefore $e_i(t) \approx 0$. Note that microgrid voltage control systems should maintain the voltages within desired ranges [12], [14]. In islanded microgrids, the maximum voltage variation margin around the voltage setpoints is usually about $\pm 10\%$ [14].

V. Simulation Case Studies

The performance of the proposed plug-and-play voltage control approach is illustrated through a case study of a DC microgrid with a mesh topology, composed of $n = 6$ DG units connected through $m = 6$ distribution lines. The topology and electrical parameters of the microgrid under study are given in Fig. 2 and Tables I-II in [5], respectively. It is assumed that a higher-level control system sends the voltage setpoints $V_1^* = 50V$, $V_2^* = 48V$, $V_3^* = 47.7V$, $V_4^* = 48V$, $V_5^* = 47.8V$, and $V_6^* = 48.1V$ to the local voltage controllers of DG units. This voltage level of $48V(\pm 5\%)$ is usually used in telecom sectors. The parameters of the weighting filters $W_i(s)$ in (6) are set as $M_i = 2$, $\omega_i^* = 80$, and $\varepsilon_i = 0.001$ for $i = 1,\dots,6$. Each DG unit is equipped with a local voltage controller $(K_i, K_{i,f})$, $i = 1,\dots,6$, designed by the convex optimization problem in (23), which is solved using YALMIP [18] and MOSEK[1]. The simulation case studies are conducted in MATLAB/Simscape Electrical environment.

A. Performance Evaluation

In order to assess the performance of the proposed line-independent PnP voltage control strategy, the following case studies are carried out: The voltage reference of DG 1 is stepped down from $50V$ to $48V$ at $t = 1s$ and stepped up to $50V$ at $t = 2s$ (*Voltage Tracking*). Next, it is assumed that DG 6 is disconnected from DC microgrid in Fig. 2 at $t = 3s$ (*PnP Functionality of DG Units*). The plug-out operation influences the dynamics of the microgrid. However, due to the line-independent feature of the proposed voltage control mechanism, it does not require to update the local voltage controllers of other DG units. Finally, the load at POI 1 is suddenly increased by 33% at $t = 4s$ (*Robustness to Load Changes*).

The transient behaviour of the DG units is depicted in Fig. 3. From Fig. 3 one can observe that the local voltage controllers track the reference setpoints with a rise time of about $0.1s$ and with no overshoot. Furthermore, the effect of voltage changes on the voltage signals of POI 2 and POI 3 is small. Moreover, the results verify that the proposed 2DOF voltage control strategy provides satisfactory transient performance in terms of robustness to uncertainties affecting the loads and the structure of the microgrids.

B. Comparison with Proposed Control Approach in [6]

In this case study, the performance of the proposed voltage control strategy is compared with the control approach in [6] for the case of constant impedance loads. To this end, it is assumed that due to a fault the line 2 connecting DG 1 to DG 3 is disconnected at $t = 5s$. The line disconnection affects the topology of DC microgrid in Fig. 2. Fig. 4 illustrates the dynamic responses of these two DG units. The results of the comparison reveal the improvements in the transient behaviour of DC microgrids by using the proposed line-independent 2DOF voltage control approach in this paper.

[1] www.mosek.com

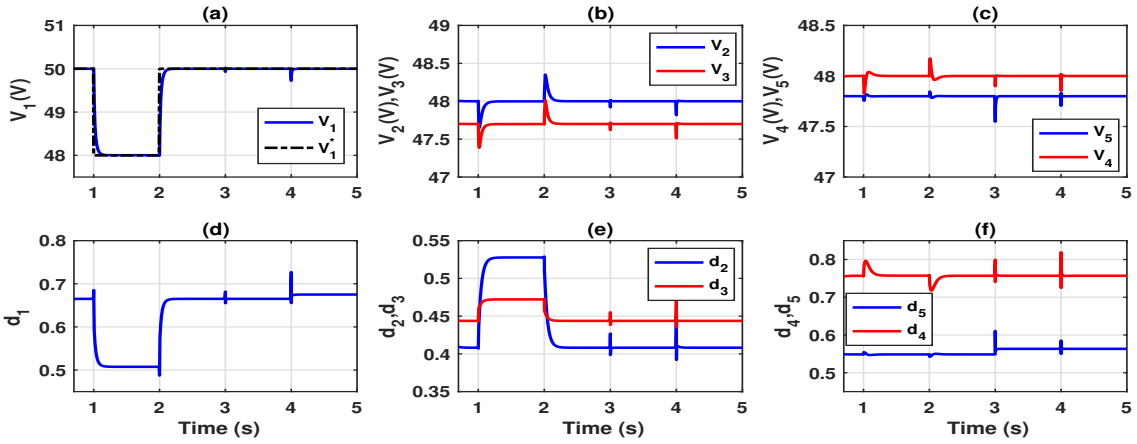

Fig. 3. Dynamic responses of DC microgrid in Fig. 2: (a) voltage at POI 1, (b) voltage at POIs 2,3, (c) voltage at POIs 4,5, (d) duty cycles of DC-DC converter of DG 1, (e) duty cycles of DC-DC converter of DG 2 and DG 3, and (f) duty cycles of DC-DC converter of DG 4 and DG 5.

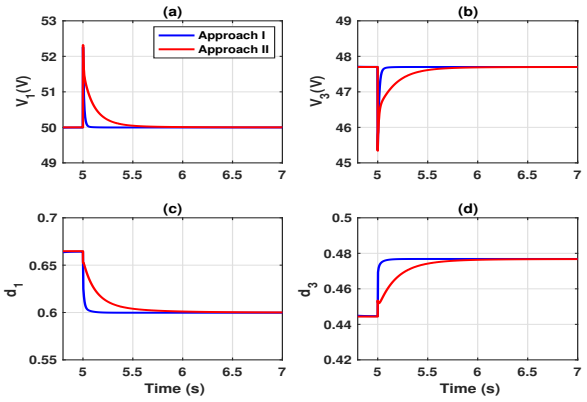

Fig. 4. Dynamic responses of DG 1 and DG 3 due to line 2 disconnection at $t = 5s$ via the proposed control approach in this letter (Approach I) and in [6] (Approach II): (a)-(b) voltage signal at POI 1 and POI 3, (c)-(d) duty cycle of DC-DC converter of DG 1 and DG 3.

VI. Conclusion

Voltage control of converter-interfaced DC microgrids is challenging due to the uncertain structure of microgrids as a result of the plug-and-play functionality of distributed generation (DG) units. In this paper, we develop a novel plug-and-play voltage control approach for microgrids with flexible structures. The proposed control strategy provides concise stability and $\mathscr{L}_2$ gain voltage tracking performance certificates for DC microgrids and facilitates the plug-and-play capabilities of DG units. Time-domain simulation case studies illustrate the feasibility and viability of the proposed voltage control strategy for DC microgrids.

References

[1] T. Dragicevic, X. Lu, J. C. Vasquez, and J. M. Guerrero, "DC microgrids– Part II: A review of power architectures, applications, and standardization issues," *IEEE Trans. Power Electronincs*, vol. 31, no. 5, pp. 3528–3549, May 2016.

[2] L. Meng, Q. Shafiee, G. F. Trecate, H. Karimi, D. Fulwani, and X. Lu, "Review on control of DC microgrids and multiple microgrid clusters," *IEEE Journal of Emerging and Selected Topics in Power Electronics*, vol. 5, no. 3, pp. 928–948, Sept. 2017.

[3] J. M. Guerrero, J. C. Vasquez, J. Matas, L. G. de Vicuna, and M. Castilla, "Hierarchical control of droop-controlled AC and DC microgrids–A general approach towards standardization," *IEEE Trans. Ind. Electron.*, vol. 58, no. 1, pp. 158–172, Jan. 2011.

[4] P. Nahata, R. Soloperto, M. Tucci, A. Martinelli, and G. Ferrari-Trecate, "A passivity-based approach to voltage stabilization in DC microgrids with ZIP loads," *Automatica*, vol. 113, pp. 1–10, 2020.

[5] M. S. Sadabadi, Q. Shafiee, and A. Karimi, "Plug-and-play robust voltage control of DC microgrids," *IEEE Trans. Smart Grid*, vol. 9, no. 6, pp. 6886–6896, Nov. 2018.

[6] M. Tucci, S. Riverso, J. C. Vasquez, J. M. Guerrero, and G. Ferrari-Trecate, "A decentralized scalable approach to voltage control of DC islanded microgrids," *IEEE Trans. Control Syst. Technol.*, vol. 24, no. 6, pp. 1965–1979, Nov. 2016.

[7] M. Tucci, S. Riverso, and G. Ferrari-Trecate, "Line-independent plug-and-play controllers for voltage stabilization in DC microgrids," *IEEE Trans. Control Syst. Technol.*, vol. 26, no. 3, pp. 1115–1123, May 2018.

[8] M. S. Sadabadi and Q. Shafiee, "Robust voltage control of DC microgrids with uncertain constant power loads," *IEEE Trans. Power Systems*, vol. 35, no. 1, pp. 508–515, Jan. 2020.

[9] ——, "Scalable PI voltage stabilization in DC microgrids," in *IFAC World Congress*, Berlin, Germany, Jul. 2020.

[10] P. Kundur, N. J. Balu, and M. G. Lauby, *Power System Stability and Control*. McGraw-Hill Professional, 1994.

[11] F. Katiraei and M. R. Iravani, "Power management strategies for a microgrid with multiple distributed generation units," *IEEE Trans. Power Syst.*, vol. 21, no. 4, pp. 1821–1831, Nov. 2006.

[12] M. Farrokhabadi, C. A. Cañizares, J. W. Simpson-Porco, E. Nasr, L. Fan, P. A. Mendoza-Araya, R. Tonkoski, U. Tamrakar, N. Hatziargyriou, D. Lagos, R. W. Wies, M. Paolone, M. Liserre, L. Meegahapola, M. Kabalan, A. H. Hajimiragha, D. Peralta, M. A. Elizondo, K. P. Schneider, F. K. Tuffner, and J. Reilly, "Microgrid stability definitions, analysis, and examples," *IEEE Transactions on Power Systems*, vol. 35, no. 1, pp. 13–29, Jan. 2020.

[13] L. I. Minchala-Avila, L. Garza-Castañon, Y. Zhang, and H. J. A. Ferrer, "Optimal energy management for stable operation of an islanded microgrid," *IEEE Transactions on Industrial Informatics*, vol. 12, no. 4, pp. 1361–1370, Aug. 2016.

[14] IEEE Std 2030.8, "IEEE standard for the testing of microgrid controllers," *IEEE Power and Energy Society*, 2018.

[15] S. Skogestad and I. Postlethwaite, *Multivariable Feedback Control Analysis and design*. Wiley, Second Edition, 2001.

[16] A. Isidori, *Lectures in Feedback Design for Multivariable Systems*. Springer, 2016.

[17] G. C. Goodwin, S. F. Graebe, and M. E. Salgado, *Control System Design*. Pearson, Prentice Hall, 2000.

[18] J. Löfberg, "YALMIP: A toolbox for modeling and optimization in MATLAB," in *Proc. IEEE Int. Symp. Comp. Cont. Syst. Design (CACSD)*, 2004. [Online]. Available: http://control.ee.ethz.ch/~joloef/yalmip.php